Vol. 160: 101–114, 2024
https://doi.org/10.3354/dao03828

DISEASES OF AQUATIC ORGANISMS
Dis Aquat Org

Published December 12

Testing for thermal acclimation in zoospores of an amphibian pathogen

Hunter M. Craig[1,*], Rima A. Stepanian[1], Kyle D. Spengler[1], Karie A. Altman[2], Jason P. Sckrabulis[3], Thomas R. Raffel[1]

[1]Department of Biological Sciences, Oakland University, Rochester, MI 48309, USA
[2]Department of Biology, St. Bonaventure University, St. Bonaventure, NY 14778, USA
[3]Department of Biological Sciences, University of Notre Dame, Notre Dame, IN 46556, USA

ABSTRACT: Thermal acclimation effects on locomotory performance have been widely documented for macroscopic organisms, but such responses remain largely unexplored in microorganisms. Metabolic theory of ecology (MTE) predicts faster responses in smaller organisms, with potential consequences for host–parasite interactions in variable temperature environments. We investigated thermal acclimation effects on zoospores of the amphibian fungal pathogen *Batrachochytrium dendrobatidis* (*Bd*), quantifying (1) thermal performance for maximum zoospore velocity and (2) high temperatures needed to immobilize 50% (CT^{50}_{max}) or 100% (CT^{100}_{max}) of zoospores. We obtained measurements within 18 min following a temperature shift. We found significant curvilinear acclimation effects on maximum zoospore velocity and CT^{50}_{max}, although the latter pattern might have been driven by confoundment with zoospore density. We also observed a significant positive effect of the trial start temperature on CT^{50}_{max}, consistent with a rapid acclimation response to the start temperature on a time scale of ~1–6 min (i.e. too rapid for our experimental acclimation treatments to detect), implying that zoospores either have constitutive heat tolerance (i.e. no acclimation) or fully acclimate CT_{max} to new temperatures within ~10 min. To explore the plausibility of such a rapid response, we analyzed published CT_{max} acclimation times for macroscopic eukaryotes, resulting in a predicted interquartile range of 3.11–25.98 min when mass-scaled to the size of a *Bd* zoospore. Taken together, these results suggest that *Bd* zoospores do exhibit thermal acclimation response on the rapid time scale predicted by MTE, possibly giving *Bd* an advantage over slower-acclimating hosts in variable-temperature environments.

KEY WORDS: Thermal acclimation · *Batrachochytrium dendrobatidis* · Chytridiomycosis · Metabolic theory of ecology · Parasite

1. INTRODUCTION

The growing threat of climate change makes it increasingly important for biologists to understand organism adaptations to temperature, including plastic responses to temperature, known as thermal acclimation responses. Thermal acclimation has been extensively researched in macroorganisms such as amphibians and insects (Rohr et al. 2018, Carilo Filho et al. 2022), but less is known about how acclimation affects performance characteristics of single-celled microorganisms. The metabolic theory of ecology (MTE) predicts that smaller organisms should have more rapid physiological responses, including thermal acclimation, due to the negative scaling relationship between body mass (M) and metabolic rate ($B \propto M^{-0.25}$; Gillooly et al. 2001, Brown et al. 2004, Raffel et al. 2013, Rohr et al. 2018). This has potentially important implications for pathogenic microorganisms, such as the amphibian fungal

*Corresponding author: hcraig@oakland.edu

pathogen *Batrachochytrium dendrobatidis* (*Bd*). The temperature variability hypothesis of Rohr & Raffel (2010) postulates that pathogens have an advantage over their hosts in variable temperature conditions, due to delays in host acclimation following unpredictable temperature shifts (Raffel et al. 2013, 2015). This hypothesis assumes that parasites have either (1) more rapid acclimation responses than their hosts or (2) constitutively expressed thermal adaptations (i.e. no acclimation responses) (Rohr & Raffel 2010, Raffel et al. 2013, 2015). Field evidence and infection experiments have found some support for the temperature variability hypothesis for *Bd* infection of amphibian hosts (Rohr & Raffel 2010, Raffel et al. 2013, 2015). However, relatively little is known about whether and how thermal acclimation responses influence metabolic or locomotory performance of microorganisms such as *Bd*, or how these responses affect the ability of pathogens to infect hosts (Raffel et al. 2013).

Thermal acclimation is a type of temperature-induced phenotypic plasticity, typically defined as within-generation changes in an organism's thermal tolerances or thermal performance curve (TPC) following experimental exposure to warm or cool temperatures (Angilletta 2009). A TPC measures quantitative changes in some performance metric across a range of temperatures within an organism's ecologically relevant thermal range (Angilletta 2009). In macroscopic organisms, thermal tolerances and performance curves are often quantified based on changes in locomotory function. For example, TPCs of amphibians are often quantified based on jumping distance or maximum velocity (Dell et al. 2014), and critical thermal maximum (CT_{max}) is often quantified as the high temperature above which frogs or salamanders fail to right themselves (Lutterschmidt & Hutchison 1997, Pottier et al. 2022). Thermal acclimation can have different effects on an organism's TPC depending on the species and how performance is measured. The beneficial acclimation hypothesis postulates that acclimation to a given temperature will increase performance at that temperature, relative to an unacclimated organism (Wilson & Franklin 2002). Consistent with beneficial acclimation, many species have improved high temperature tolerance (i.e. increased CT_{max}) following extended exposure to warm temperature (Rohr et al. 2018). However, beneficial acclimation is not universal, especially for TPC changes within an organism's normal temperature range (Huey et al. 1999, Wilson & Franklin 2002). Other common acclimation patterns include 'cooler is better' or 'warmer is better' effects, in which the TPC is overall higher following acclimation to cooler or warmer temperatures, or 'optimal temperature' effects, in which the TPC is higher following acclimation to an intermediate temperature (Wilson & Franklin 2002, Altman et al. 2016, McWhinnie et al. 2021). In principle, an organism could also have constitutive rather than induced adaptations to temperature variation, in which case there would be no measurable effects of experimental acclimation treatments on an organism's thermal tolerances or TPC.

Relatively few studies have investigated within-generation thermal acclimation responses in microorganisms (but see Robinson & Morris 1984, Addy et al. 1998, Robinson 2001, Heinemeyer et al. 2006, Malcolm et al. 2009, Crowther & Bradford 2013). This might be partly because such acclimation effects should only be detectable during a short window of time following an experimental shift in temperature, making them difficult to study (Rohr et al. 2018). According to MTE, biological process times (t_b) including time to acclimation should increase with organism body mass according to a quarter-power scaling relationship ($t_b \propto M^{0.25}$; Gillooly et al. 2001). Rohr et al. (2018) found indirect evidence for this scaling relationship, showing that acclimation effects on CT_{max} were more likely to be detected in small animals such as stoneflies (2.0×10^{-5} kg) when ramping trials were conducted with faster heating rates (i.e. shorter measurement times). Thus, we are more likely to detect thermal acclimation if the measurement is collected soon after shifting an organism to a new temperature. Most studies of 'thermal acclimation' in single-celled microorganisms have been conducted on time frames of days to weeks, measuring changes in thermal tolerances or TPCs over multiple generations (Bennett & Lenski 1997, Hall et al. 2010, Tian et al. 2022, Tveit et al. 2023). Although these responses are likely to represent a type of multi-generational phenotypic plasticity in some cases (Bennett & Lenski 1997), we cannot entirely rule out the possibility that these effects were caused by genetic evolution rather than a classic thermal acclimation response. Indeed, some of these authors explicitly define 'thermal acclimation' as encompassing both phenotypic plasticity and genetic evolution (Tian et al. 2022, Tveit et al. 2023). This focus on longer time scales and evolutionary responses might be in part because microbial performance is often quantified based on population growth rates in culture or competitive ability, precluding within-generation measurements (although respiration is also commonly measured; Bennett & Lenski 1997, Malcolm et al. 2009, Hall et al. 2010, Crowther & Bradford 2013, Tian et al. 2022, Tveit et al.

2023). A number of studies have documented thermal acclimation responses in fungi based on various performance metrics (e.g. radial growth of hyphal cultures) (Robinson & Morris 1984, Ouedraogo et al. 1997, Fargues et al. 1997, Vidal et al. 1997, Addy et al. 1998, Robinson 2001, Heinemeyer et al. 2006, Malcolm et al. 2009, Dell et al. 2013, Crowther & Bradford 2013). However, to our knowledge, no empirical studies have directly tested for within-generation thermal acclimation effects on thermal tolerances or TPCs of single-celled microbes with independently motile cells. Our lack of data for acclimation effects on microbe locomotory performance is a particularly important knowledge gap, due to the likely association between infective stage velocities and pathogen infectivity (e.g. *Bd* zoospores; Canter & Jaworski 1981, Appiah et al. 2005). Much of what we know about microorganism thermal responses comes from studies of changes in gene transcription and heat shock protein expression (Schlesinger et al. 1982, Alcina et al. 1988, Kalinina et al. 1988, Krobitsch et al. 1998, Fang & McCutchan 2002, Engstler & Boshart 2004), but these are not direct measures of organism performance.

In the current study, we tested for thermal acclimation effects on high-temperature thermal tolerance and thermal performance of *Bd* zoospores in culture, focusing on performance metrics that could be quantified soon (within 20 min) after removing zoospores from 1 of 3 acclimation temperatures (i.e. hopefully before zoospores could become fully acclimated to the new 'performance' temperature). To quantify changes in heat tolerance, we used the ramping method to quantify temperatures at which 50 or 100% of visible zoospores stopped swimming (CT^{50}_{max} and CT^{100}_{max}, respectively). To quantify changes in thermal performance, we measured the maximum velocity of zoospores at 1 of 8 performance temperatures using video microscopy. We also fit MTE-based models of thermal performance to the zoospore velocity data to obtain estimates of *Bd* metabolic activation energy (E_a), a key metabolic parameter (Molnár et al. 2017). To explore MTE predictions for thermal acclimation times in microorganisms, we analyzed published values for acclimation times in potential amphibian hosts of *Bd* and generated predicted times for an organism the size of a *Bd* zoospore. Based on the beneficial acclimation hypothesis, we predicted that CT^{50}_{max} and CT^{100}_{max} measurements would be higher following warm temperature acclimation, and that zoospore velocities would be faster at a given temperature if they had recently been acclimated to that temperature.

2. MATERIALS AND METHODS

2.1. Culturing *Bd*

Bd strain JEL423, isolated from *Peltophryne lemur* in 2004 (Farrer et al. 2011), was obtained from Joyce Longcore in 2016 and grown in 1% tryptone broth for approximately 10 generations prior to long term −80°C storage as frozen stocks (Boyle et al. 2003). We used all *Bd* within 1 mo after thawing from stock, to minimize evolutionary changes in response to culture conditions (Voyles et al. 2014, Kumar et al. 2020). Prior to each experimental trial, we thawed and grew *Bd* in sterile 1% tryptone broth solution for 1 wk at 21°C. Next, 500 µl of this culture were spread onto each of several sterile 1% tryptone agar plates and grown for 1 wk at 21°C. We placed each plate into an Exo Terra reptile egg incubator (Model PT2445, Hagen) or a commercial countertop beverage center (Model SCR114L, Summit Commercial, Felix Storch) to achieve lower temperatures, set to low, middle, and high acclimation temperatures (9, 16.5, 24°C), and allowed the plate to grow for 3 d. For both experiments, 6 acclimation incubators were arranged in a randomized block design with 2 incubators per temperature treatment. We used digital aquarium thermometers to confirm that actual temperatures were near our target temperatures and used Onset HOBO loggers to record acclimation temperature readings in the incubators every 30 min. We calculated the mean HOBO temperature throughout each acclimation period for use in analyses. At the end of a 3 d acclimation period, each plate was flooded with 3 ml artificial spring water (Cohen et al. 1980) that had been pre-equilibrated to the acclimation temperature. The flooded plate remained in the acclimation incubator for another 20 min to allow zoosporangia to release zoospores into the water.

2.2. Measuring zoospore critical thermal maximum

To measure zoospore CT^{50}_{max} and CT^{100}_{max}, we conducted temperature ramping trials by placing samples on a microscope slide fitted into a Stage Top incubation chamber (system by Okolab SRL). Prior to beginning the ramping trial, we cleaned the slide with chilled 70% ethanol, cooling the slide to a target temperature of 20°C. After the ethanol was fully dry, we transferred 20 µl of sample from the flooded agar plate (described in Section 2.1) to the slide and inserted the Oko machine's miniature

temperature probe directly into the sample droplet to measure temperature in real time. It was difficult to achieve a precise trial start temperature for every trial, so the start temperature varied between 15 and 25°C. We recorded the start temperature for each trial, allowing us to investigate start temperature as a potentially important covariate (Terblanche et al. 2007).

We then sealed the top stage incubation chamber and positioned it over the objective lens of an inverted Nikon Diaphot compound microscope at 200× magnification. We recorded the approximate zoospore density (zoospores per field of view) and proportion of zoospores moving based on an observer estimate. To begin the ramping process, a second investigator turned on the stage heater, resulting in gradual heating of the sample at a rate of approximately 1.8°C min^{-1} (range of 0.8–2.8°C min^{-1}). The observer watched the zoospores continuously throughout the ramping trial and noted times when 50% (CT^{50}_{max}) and 100% (CT^{100}_{max}) of the zoospores had stopped moving. A second investigator recorded the stage temperature at these times. It took approximately 30 s to set up for each ramping trial, after which it took 2.5 ± 1.2 min (mean ± SD) to reach CT^{50}_{max} and 8.5 ± 4.7 min to reach CT^{100}_{max}, corresponding to total times since removal from acclimation temperature of 3 and 9 min, respectively.

An advantage of using real-time observations in lieu of video analysis for CT_{max} measurements was that it allowed us to observe zoospore movement based on the full field of view and variable focal depth. However, it increased the risk that subjective judgments of observers might influence the results. To control for potential differences among observers, both observers went through a training period to confirm that their estimates correlated with estimates by the first author. To control for effects of observer bias on zoospore density, proportion moving, and CT_{max} estimates, observers were blinded to acclimation treatment and current temperature readings. To verify the consistency of observer zoospore density estimates, we conducted a follow-up image analysis from a subset of trials (temporal blocks E–J). We obtained photos using a GoPro fitted into the ocular lens of the microscope. The GoPro did not record the entire field of vision nor depth of focus that we observed manually, resulting in lower numbers of zoospores being visible in photographs; nevertheless, this allowed us to confirm that our observer estimates were positively correlated with an objective alternative measure of zoospore density ($r = 0.786$, $df = 23$, $p < 0.001$).

2.3. Measuring zoospore velocity

To measure velocity at various performance temperatures, for each of 6 temporal blocks, we collected water containing zoospores from flooded agar plates (described above) grown at each acclimation temperature (targets of 9, 16.5, or 24°C). We transferred a sub-sample to a microtube, vortexed it, and used a hemacytometer to quickly determine the density of zoospores from each agar plate culture. We then diluted each inoculum with water (already equilibrated to the acclimation temperature) to a target concentration of 15 zoospores nl^{-1}. When *Bd* cultures did not produce enough zoospores for 15 zoospores nl^{-1}, we used a minimum concentration of 7 zoospores nl^{-1}, resulting in zoospore concentrations between 7 and 15 zoospores nl^{-1}. To verify that zoospore concentration did not affect the velocity results, we tested for an effect of zoospore concentration in our final statistical model. Within each temporal block, we selected a single culture to use as the inoculum source for each of the 3 acclimation temperature treatments. From each selected inoculum culture, we made up to 4 aliquots of 1 ml of diluted inoculate in 1.5 ml microcentrifuge tubes (hereafter 'test samples') to be tested at different performance temperatures randomly selected from 1 of 8 target temperature treatments (7, 10, 13, 16, 19, 22, 25, 28°C). We analyzed 8 test samples within a given temporal block (except for the final block, when we tested 12 samples), analyzing 2–4 test samples from each inoculum culture. For later temporal blocks, randomizations were constrained to increase replication for performance × acclimation temperature treatment combinations with lower numbers of replicates, aiming to generate high-quality data for at least 2 replicate test samples for a given treatment combination while ensuring high interspersion of temperature treatments within a given block. Some replicates were lost due to failure of cultures to generate sufficient live zoospores or failure to obtain high-quality videos. Zoospores were slightly older for test samples analyzed later within each temporal block. To reduce this source of experimental error, we randomized the order of acclimation and performance treatments tested within each block and ensured that all test samples were analyzed within 3 h of flooding the plate.

We were unable to use a stage heater to maintain temperatures during microscopy for this experiment, because the available stage heater only allows for temperature set points of >25°C. Instead, we placed each test sample into a performance incubator set to

1 of the 8 target performance temperatures. Nine performance incubators were arranged in a randomized block design, with temperature treatments re-randomized for each of 6 temporal blocks of the experiment. After allowing 10 min to ensure each tube was fully equilibrated to the new performance temperature, 40 µl were transferred to a hemacytometer and cover-slipped for video microscopy. To help maintain the target performance temperature throughout video microscopy, the thermal inertia of each hemacytometer was increased by placing it within a foam cutout on top of a 150 mm diameter Petri dish filled with gel wax (Fig. S1 in the Supplement at www.int-res.com/articles/suppl/d160p101_supp.pdf). The gel wax Petri dish was equilibrated to the performance temperature prior to each trial. Each replicate was recorded 3 times for 10 s at 400× magnification using a Leica DM 1000 microscope, a Leica DFC450 C digital microscope camera, and VirtualDub screen recording software (www.virtualdub.org). We obtained nearly all videos within 15 min after moving zoospores from their original acclimation temperature to their new performance temperature, for a mean time of 14.7 ± 1.0 min (SD) at the new performance temperature prior to obtaining measurements. Hemacytometers gradually equilibrated to room temperature during video microscopy, but we were unable to measure continuous changes in sample temperature during trials. To obtain better estimates of real-time temperature at the time of each video, we conducted a separate experiment to determine the rate at which hemacytometers equilibrated to room temperature from a given start temperature. Samples of 40 µl of water were taken from incubators set to 9, 16.5, or 24°C, and placed onto a gel-wax-stabilized hemacytometer at the same temperature as described above. The miniature temperature probe used in the CT_{max} ramping measurements was then placed into the water sample and a cover slip was laid on top. The gel wax block and hemacytometer were placed on a microscope stage to simulate a video microscopy session, and hemacytometer temperature was recorded every minute for 10 min. We used nonlinear least squares to fit the data to the following equation:

$$T\{t\} = T_R + (T_0 - T_R)^{-rt} \quad (1)$$

where T is sample temperature (in °C) as a function of time, T_R is room temperature, T_0 is the initial performance temperature (mean of the 3 most recent HOBO logger measurements in the performance incubator), r is the rate of increase or decrease in temperature, and t is the time in minutes since the sample was removed from the performance incubator (Newton's law of cooling; Lienhard & Lienhard 2020; Fig. S2). Room temperature was a consistent average of 21.6°C and was assumed constant in the model, making r the only free parameter with an estimated value of 0.048 ± 0.001 SE. We used this model to estimate the real-time hemacytometer temperature for each video from the primary zoospore velocity experiment, based on the start (incubator) temperature and the time since each sample was taken from its performance incubator.

We analyzed zoospore velocity videos using the 'wrMTrck' plug-in (Table S1; Pedersen 2011) for ImageJ (Schneider et al. 2012), recording the mean velocity of the fastest zoospore from each video. Each video was manually checked to confirm that the wrMTrck software accurately tracked at least the fastest 10 zoospores for at least 1 s and did not re-label the zoospores during zoospore collisions or when a zoospore moved out of the frame of view. We also recorded the estimated proportion of zoospores moving in each video. The unit of replication for statistical analysis was the individual test sample, for which there was only a single replicate per performance temperature from a given inoculum culture. Prior to statistical analyses, we calculated the average maximum velocity from the 3 videos for each replicate test sample. We also recorded the estimated proportion of zoospores moving in each video. We did not use videos if they were out of focus, or if the software did not accurately track zoospores.

2.4. Analysis of experimental data

All statistical analyses and models were implemented in Program R Version 4.0.3 (R Core Team 2020). CT_{max} and zoospore velocity data were analyzed using linear regression models (function 'lm'), with variable significance evaluated with Type II F-tests using the 'Anova' function from the 'car' package (Fox & Weisberg 2019), and models were selected using backward selection starting with full models including all possible quadratic and interactive effects of acclimation and performance temperature. None of the final models violated the assumption of homoscedasticity or had influential outliers as determined by Cook's distance. Residuals were approximately normal based on Q-Q plots and Shapiro-Wilk tests (all $p > 0.2$), except for the CT_{max}^{50} model due to the presence of 2 non-influential outliers. When these 2 datapoints were removed, the CT_{max}^{50} residuals were approximately normal ($W = 0.982$, $p = 0.759$) and results were unchanged from those presented in Table 1.

Table 1. Model outputs for *Batrachochytrium dendrobatidis* zoospore performance (maximum zoospore velocity and critical thermal maximum). The first 2 models included effects of acclimation temperature, start temperature, and zoospore density (zoospores per field of view at 200× magnification) on critical thermal maximum with 50% immobility and 100% immobility (CT_{max}^{50} and CT_{max}^{100}, respectively). Each model presented here was simplified by backward stepwise selection to remove non-significant predictors, from an initial full model including all possible quadratic and interactive effects of acclimation and performance temperature treatments. To allow interpretation of main effects, *F*-statistics were calculated using Type II sums of squares and variables included in quadratic terms were centered around zero

Response	Predictor	*F*	df	p
CT_{max}^{50}	Acclimation temperature	1.1	1, 44	0.292
	Start temperature	4.6	1, 44	0.038
	Zoospore density	4.5	1, 44	0.039
CT_{max}^{100}	Acclimation temperature	0.4	1, 46	0.553
	Start temperature	3.0	1, 46	0.092
	Zoospore density	16.2	1, 46	<0.001
Velocity	Performance temperature	150.9	1, 37	<0.001
	(Performance temperature)^2	9.4	1, 37	0.004
	Acclimation temperature	1.2	1, 37	0.278
	(Acclimation temperature)^2	4.8	1, 37	0.034
	Performance temperature × Acclimation temperature	0.4	1, 37	0.553
	(Performance temperature)^2 × Acclimation temperature	6.4	1, 37	0.015

For the CT_{max} experiment, the primary explanatory variables we tested were acclimation temperature and start temperature. Zoospore density varied among replicates, so we also tested models with and without zoospore density as a covariate. CT_{max}^{50} and zoospore density appeared curvilinear with respect to acclimation temperature, so we tested for quadratic effects of acclimation temperature on these variables, centering acclimation temperatures around zero to avoid marginality errors. We noted 1 datapoint with an excessively high zoospore density, as well as 5 datapoints that had only 50–60% zoospores initially moving. Out of concern that these data might not be fully comparable to other datapoints, we ran our final models with and without these data included.

For zoospore velocity measurements, we used polynomial regression to test for linear and quadratic effects of acclimation temperature and performance temperature, as well as the interaction between acclimation temperature and performance temperature. The purpose of the interaction term was to test the beneficial acclimation hypothesis, which predicts a positive interaction between these variables (Altman et al. 2016). These regression models included a quadratic effect of performance temperature to account for curvilinearity of the TPC. For the purposes of this analysis, both acclimation and performance temperatures were centered around zero to avoid marginality problems when interpreting linear terms.

2.5. Analysis of literature data — acclimation times for amphibian hosts of *Bd*

To explore MTE predictions for acclimation times at the scale of a zoospore, we analyzed thermal acclimation times from the published literature for 3 eukaryotic taxa: amphibians, arthropods, and fish. We used 18 articles that measured the timing of acclimation effects on CT_{max} (loss of righting response, onset of spasms, heat rigor, or similar cessation-of-movement responses; Tsukuda 1960, Hutchison 1961, Brattstrom & Lawrence 1962, Brattstrom & Regal 1965, Brattstrom 1970, Hutchison & Ferrance 1970, Hutchison et al. 1973, Hutchison & Rowlan 1975, Cossins et al. 1977, Claussen 1977, 1980, Chung 1981, Layne & Claussen 1982a,b, Lagerspetz & Bowler 1993, Bennett et al. 1998, Allen et al. 2012, Fangue et al. 2014). Time to full acclimation was defined in this analysis as the time it took for CT_{max} to equilibrate to a new value following a temperature shift (see Fig. S3) based on overlap of standard deviation bars, mean–range overlap, or our best estimate of equilibrium when error bars were not provided. We attempted to standardize this procedure across studies and therefore our equilibrium criteria sometimes resulted in slightly different time-to-acclimation measurements than was reported in the source studies. A single 'measurement' was defined as time to full acclimation for a single combination of temperature treatments within an acclimation experiment (Fig. S3). If CT_{max} had not equilibrated by the end of an experiment, we assumed time to acclimation was greater than the duration of the experiment and recorded this as the minimum time to full acclimation. If body mass was not available from within the same published study, we used species mass estimates from the AmphiBIO database (Oliveira et al. 2017) or from other published sources of the same species and life stage (Rabb 1958, Nickerson & Mays 1973, Fitzpatrick 1973, Gatz & Piiper 1979, Arakelova 2001, Szczerbowski 2001, Urrejola et al. 2011, Zaibel et al. 2019, Bruce 2022). We then scaled down each acclimation time to an organism the size of a zoospore (diameter = 4 µm; Longcore et al. 1999) using survival analysis (Therneau 2001) with censoring based on whether or not the species achieved full acclimation. We used the following series of equations to generate acclimation

time predictions. Gillooly et al. (2001) assumed that biological times (such as time to full acclimation) are proportional to body mass to the quarter power:

$$t_b \propto M^{0.25} e^{E_a/kT} \quad (2)$$

where t_b is biological time, M is mass, E_a is activation energy (= E_i in Gillooly et al. 2001), k is Boltzmann's constant, and T is temperature in degrees K. Focusing on the mass-scaling part of the equation, process time should be approximately equal to $M^{0.25}$ multiplied by some constant (C; Eq. 3), and we can rearrange this equation to show that this constant should be approximately equal to mass-scaled process times (Eq. 4):

$$t_b \cong C \cdot M^{0.25} \quad (3)$$

$$t_b \cdot M^{-0.25} \cong C \quad (4)$$

We used censored survival analysis (function 'survreg' from the 'survival' package; Therneau 2001) to estimate predicted values of C across all literature values for time to full acclimation, using the mass-scaled acclimation times as the end time response variable and censoring any measurements where animals were not fully acclimated by the end of the published experiment. Censoring these measurements allows us to account for uncertainty due to published experiments not being long enough to detect time to full acclimation. We selected a Weibull waiting time distribution based on AIC comparisons. We used the 'predict' function to generate predicted median, interquartile range, and 95% prediction intervals for C. Then we entered these predicted C values into Eq. (4) to generate predicted times to full acclimation for organisms of different body masses, focusing on the geometric mean body mass for all measurements in our literature review (3.08 g) and the body mass of an individual zoospore (3.35×10^{-11} g), assuming zoospores are spheres with a density approximately equal to that of water.

3. RESULTS

3.1. Critical thermal maximum results

Half of the *Bd* zoospores became immobile (CT^{50}_{max}) at 26.59 ± 2.27°C (SD; range 22–32°C) and 100% were immobile at 31.71 ± 2.89°C (range 25–37°C; Fig. 1). There was an apparent curvilinear effect of acclimation temperature on both measures of thermal tolerance, especially CT^{50}_{max} (Fig. 1). Zoospores acclimated to middle temperatures (16.5°C) appeared to exhibit higher CT^{50}_{max} values than those acclimated to low (9°C) or high temperatures (24°C; Fig. 1). When tested alone, acclimation temperature had a significant quadratic effect on CT^{50}_{max} ($F_{1,45} = 5.8$, p = 0.021); however, this effect became nonsignificant when zoospore density and start temperature were added to the model ($F_{1,43} = 0.6$, p = 0.430). There was no significant quadratic effect of acclimation temperature for CT^{100}_{max} ($F_{1,47} = 1.1$, p = 0.293). We therefore left quad-

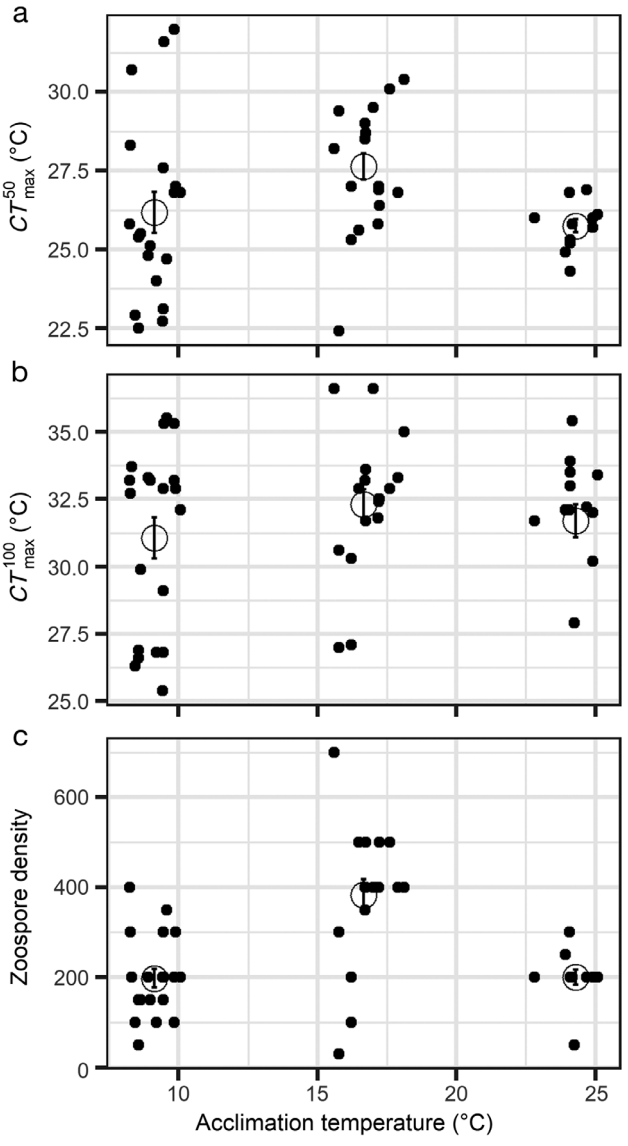

Fig. 1. *Batrachochytrium dendrobatidis* (*Bd*) zoospore critical thermal maximum and density estimates (zoospores per field of view at 200× magnification) plotted as a function of acclimation temperatures. Open circles represent the mean critical thermal maximum at (a) 50% immobility (CT^{50}_{max}) and (b) 100% immobility (CT^{100}_{max}), and (c) zoospore density of each acclimation treatment with standard error bars. Closed circles represent the individual measurements, plotted at their actual acclimation temperatures as measured by HOBO loggers

ratic effects of acclimation temperature out of final CT_{max} models presented in Table 1. There was no significant linear effect of acclimation temperature on CT^{50}_{max} or CT^{100}_{max} in any of these models (all p-values >0.05; Table 1).

Start temperature had a significant positive effect on CT^{50}_{max} and a nonsignificant trend toward a positive effect on CT^{100}_{max} (Table 1, Fig. 2). Zoospore density had significant positive effects on both CT^{50}_{max} and CT^{100}_{max} (Table 1, Fig. 2). Whether zoospore density was included in these models did not qualitatively change the effects of start temperature on CT^{50}_{max} or CT^{100}_{max}. There was a curvilinear effect of acclimation temperature on zoospore density ($F_{1,47} = 27$, $p < 0.001$), similar to the apparent curvilinear effect of acclimation temperature on CT^{50}_{max} (Fig. 1). We tried running models with and without datapoints with unusually high zoospore densities, low proportion moving, or high heating rates (1 sample with zoospore density >550 per field of view, 5 samples with <70% of zoospores moving, and 1 sample with a heating rate >4°C min^{-1}). Removing these datapoints did not qualitatively change the effects of acclimation temperature or zoospore density, but start temperature effects became more pronounced (CT^{50}_{max} $F_{1,38} = 11.8$, $p = 0.001$; CT^{100}_{max} $F_{1,39} = 4.9$, $p = 0.033$).

3.2. Zoospore velocity results

Zoospore velocities increased with performance temperature (Table 1, Fig. 3) and appeared to level off

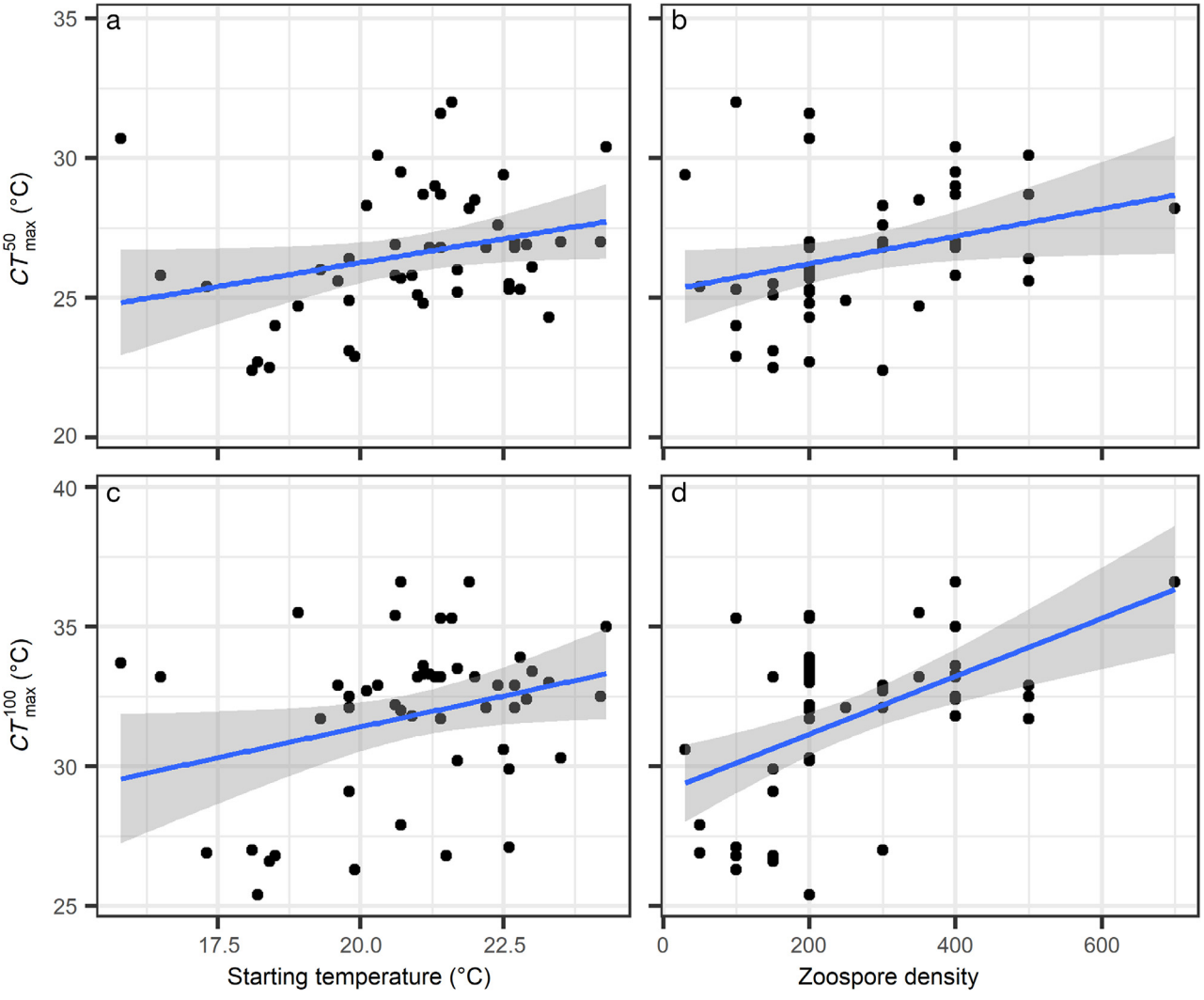

Fig. 2. Effects of (a,c) trial start temperature and (b,d) zoospore density (zoospores per field of view at 200× magnification) on *Bd* zoospore critical thermal maximum with 50% immobility (CT^{50}_{max}; a,b) and 100% immobility (CT^{100}_{max}; c,d). Trendlines show linear model fits and 95% CI bands

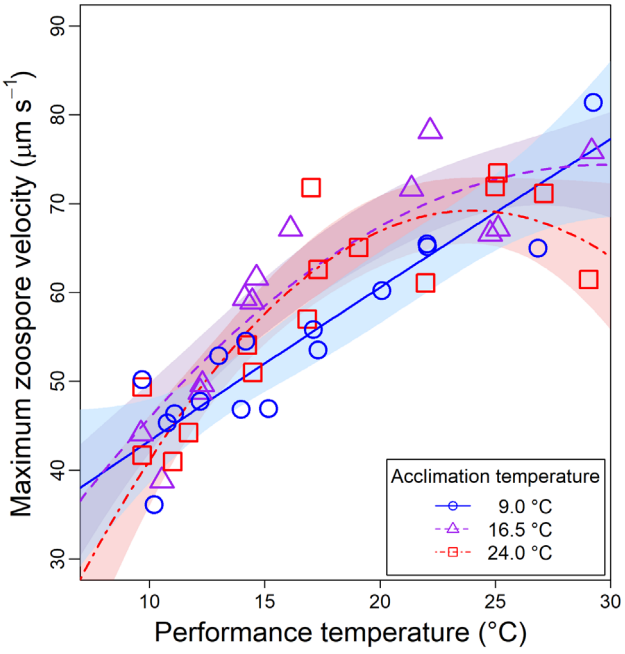

Fig. 3. Thermal performance curves showing maximum *Bd* zoospore velocity (μm s^{-1}) as a function of performance temperature (°C). The curves show predictions for each acclimation treatment with 95% CI bands, based on the full model presented in Table 1

at higher temperatures, resulting in a curvilinear pattern with peak zoospore velocities between 22 and 29°C (Fig. 3). The curvilinearity of the performance curve was supported by a significant quadratic effect of performance temperature on maximum zoospore velocity (Table 1). There was no significant main (linear) effect of acclimation temperature on maximum zoospore velocity; however, there was a significant quadratic effect of acclimation temperature (Table 1) reflecting a curvilinear pattern whereby cool-acclimated zoospores had lower velocities at intermediate performance temperatures (~13–22°C) whereas middle- and warm-acclimated zoospores had similarly high velocities in this range (Fig. 3). There was also a significant interaction between acclimation temperature and the quadratic effect of performance temperature (Table 1), reflecting a change in the curvature of the performance temperature effect where the cool acclimation treatment had markedly less (or even slightly opposite) curvature relative to the middle and warm acclimation treatments (Fig. 3). The initial proportion of zoospores moving had no significant relationship with either maximum zoospore velocity ($F_{1,42}$ = 1.8, p = 0.188) or performance temperature ($F_{1,42}$ = 0.4, p = 0.526), and there was no significant relationship between zoospore concentration and maximum zoospore velocity ($F_{1,42}$ = 0.01, p = 0.917).

3.3. MTE predictions for zoospore acclimation times (literature data analysis)

We reviewed measurements of time to full acclimation for amphibians, arthropods, and fish from 18 published papers (Tsukuda 1960, Hutchison 1961, Brattstrom & Lawrence 1962, Brattstrom & Regal 1965, Brattstrom 1970, Hutchison & Ferrance 1970, Hutchison et al. 1973, Hutchison & Rowlan 1975, Cossins et al. 1977, Claussen 1977, 1980, Chung 1981, Layne & Claussen 1982a,b, Lagerspetz & Bowler 1993, Bennett et al. 1998, Allen et al. 2012, Fangue et al. 2014), generating 156 measurements from 38 species as described in Section 2.5 and in Fig. S3. The number of individual animals included in each measurement was not always available. Here, 'measurement' refers to a single combination of temperature treatments in a CT_{max} acclimation experiment. Body masses ranged from 0.05 to 467.8 g, but the vast majority of organisms in the literature were small, with an overall geometric mean of 3.08 g. The survival analysis model predicted a median time to full acclimation of 3.90 d across all organisms so far quantified, with an interquartile range of 1.19–9.94 d (95% prediction interval of 0.04–37.22 d). Scaling our predictions down to a *Bd* zoospore, the model generated a median prediction of 10.20 min with an interquartile range of 3.11–25.98 min (95% prediction interval of 0.12–97.31 min). While an extensive meta-analysis of acclimation times for all eukaryotes would be a more rigorous way to generate predictions for acclimation times of a microscopic fungus, this was beyond the scope of our study.

4. DISCUSSION

We did not find clear evidence that experimental acclimation treatments affected CT_{max}^{50} or CT_{max}^{100}. However, we did find evidence of a complex curvilinear effect of acclimation temperature on maximum zoospore velocity, where cool-acclimated zoospores were slower than middle- or warm-acclimated zoospores when measured at intermediate performance temperatures (~13–22°C; Fig. 3). The velocity performance curves converged at ~9–11°C, at which temperature there was no discernable acclimation effect on zoospore velocity (Fig. 3). This pattern is consistent with a beneficial acclimation response at warmer acclimation temperatures, at least if we focus on performance temperatures below ~23°C (Fig. 3). These results suggest that cool-acclimated *Bd* zoospores have different locomotory performance char-

acteristics than zoospores acclimated to warmer temperatures. Assuming this reflects a real pattern, these results further imply that full acclimation of *Bd* locomotion to a new temperature takes longer than the ~15 min it took for us to obtain our video measurements. However, loss of datapoints due to poor video quality led to fewer replicates than we intended of the cool-acclimation treatment at intermediate performance temperatures, and we should be cautious in interpreting quadratic effects with $p > 0.01$ as clear evidence of thermal acclimation responses. It would be interesting to see if these patterns can be replicated in future studies of thermal acclimation effects on microbial motility.

The lack of clear acclimation effects on CT_{max} suggests that zoospores either (1) had constitutive responses to temperature when it comes to heat tolerance or (2) fully acclimated their CT_{max} to new temperatures before we were able to complete our measurements (i.e. ~3 min for CT^{50}_{max}, ~9 min for CT^{100}_{max}). However, ramping trials with higher start temperatures had significantly higher CT^{50}_{max}. Start temperature effects are commonly observed in studies that use ramping trials to measure critical thermal limits (Terblanche et al. 2007, Kingsolver & Umbanhowar 2018). While start temperature effects remain poorly understood, they might represent full or partial acclimation responses occurring on short time scales. The positive effect of start temperature on CT^{50}_{max} observed in the current study is consistent with the beneficial acclimation hypothesis, but only if zoospore acclimation occurs very rapidly. Zoospores were only at or near the start temperature for the first ~30 s of the ramping trial, and most CT^{50}_{max} measurements were completed in under 3 min, so any acclimation effects caused by exposure to the start temperature would have occurred in less than a minute.

Such a rapid thermal acclimation response might be plausible for an organism as small as a *Bd* zoospore. Our literature analysis of acclimation times for various eukaryotic species (masses 0.05–467.8 g) found that most took ~1–10 d to fully acclimate their CT_{max} to a new temperature (interquartile range of 1.19–9.94 d), which, when scaled down to the size of a zoospore (assuming a quarter-power mass scaling relationship), translates into a probable acclimation time of ~3–26 min. The predicted median time to full acclimation (10.20 min) implies that 50% of microorganisms at this size should fully acclimate to a new temperature within ~10 min following a temperature shift, possibly accounting for our failure to detect effects of experimental acclimation treatments on CT_{max} measurements that took 1–18 min to complete. However, even these numbers might underestimate the rate at which zoospores could acclimate to new temperatures. Increased thermal tolerances referred to as 'heat hardening' effects have been documented in some amphibian species (e.g. *Xenopus laevis* juveniles) after brief exposure to elevated temperatures (10 min followed by 2 h room temperature interval for *X. laevis* study; Spotila et al. 1989, Sherman & Levitis 2003). Assuming the juvenile *X. laevis* masses were approximately ~3.5 g, a 2.2 h heat hardening time scale translates to 0.23 min when scaled down to the size of a *Bd* zoospore. Short thermal response time frames have been observed in other microscopic eukaryotes, including yeasts, amoebae, and kinetoplastid flagellates, that showed changes in heat shock protein expression in as few as 10–30 min following a temperature shift (Finkelstein & Strausberg 1982, Loomis & Wheeler 1982, Alcina et al. 1988, Kalinina et al. 1988, Krobitsch et al. 1998). Although this is not a direct measure of organism performance, heat shock proteins are generally assumed to protect cells from high temperature stress (Bakthisaran et al. 2015, Ikwegbue et al. 2017). Altered heat shock protein expression has been observed as quickly as 1–15 min (i.e. <1 generation) following a temperature shift in bacteria (Neidhardt et al. 1982, Pellon et al. 1982, Travers & Mace 1982, Yamamori et al. 1982). Vector-borne parasitic protozoans of humans have been found to exhibit significant changes in gene transcription within 1–4 h following a sudden shift to a new host body temperature (Fang & McCutchan 2002, Engstler & Boshart 2004). Taken together, these findings suggest that single-celled organisms likely do exhibit classic acclimation responses (i.e. within-generation plasticity) and that these might occur on the rapid time scales predicted by MTE.

It is possible that we only observed start temperature effects on CT^{50}_{max} because these data were collected within 3 min of exposure to a particular start temperature, whereas CT^{100}_{max} measurements took ~9 min to complete, by which time start-temperature effects had mostly dissipated (although start temperature became a significant predictor of CT^{100}_{max} after removing some data points with extreme values for high zoospore density, low proportion moving, and high heating rate). Follow-up experiments would be necessary to confirm rapid *Bd* zoospore acclimation in response to an experimental acclimation treatment, perhaps with a much higher rate of temperature increase to complete ramping trials in under 1 min.

There appeared to be a curvilinear effect of acclimation temperature on CT^{50}_{max} that would have been consistent with an 'optimal temperature' acclima-

tion response (Fig. 1). However, this pattern appears to have been caused by a confoundment between our CT^{50}_{max} and zoospore density, and the quadratic effect of acclimation temperature became nonsignificant when zoospore density was added to the model (Fig. 1, Table 1). Zoospore density also had a curvilinear relationship with acclimation temperatures, with higher zoospore densities collected from cultures that were grown at an intermediate acclimation temperature of 16.5°C. This is close to the optimal temperature range for *Bd* growth in culture (Piotrowski et al. 2004), which might account for higher zoospore production. Observers might have overestimated CT^{50}_{max} when zoospores were denser because it was more difficult to accurately estimate the proportion of zoospores moving. Zoospore density was also a positive predictor of CT^{100}_{max}, although there was no significant quadratic effect of acclimation temperature on this response variable. CT^{100}_{max} measurements should have been less subject to observer bias, but a positive effect of zoospore density makes biological sense because observing a larger number of zoospores increases the probability of at least 1 zoospore continuing to move as the temperature is ramped up. Another potential source of experimental confoundment is that zoosporangia develop at temperature-dependent rates (Woodhams et al. 2008), which might result in different distributions of zoosporangia developmental stages or different age distributions of released zoospores in different acclimation treatments. We tried to limit this course of experimental error by waiting until the end of the acclimation period to flood plates with water, to encourage the release of fresh zoospores, but controlling for zoosporangium developmental rates might be useful in future experiments.

Our overall measurements of *Bd* zoospore thermal tolerances, and the thermal performance curves for maximum zoospore velocity, were consistent with aspects of *Bd* thermal biology measured in prior studies (Stevenson et al. 2013, Voyles et al. 2017). Half of the zoospores became immobile at 26.59 ± 2.27°C (SD) and 100% became immobile at 31.71 ± 2.89°C. These CT_{max} values correspond well with the known thermal limits of *Bd*, with 27°C often cited for zero growth in culture (Longcore et al. 1999, Piotrowski et al. 2004) and 30°C sometimes used as a target temperature for heat treatments to clear frogs of *Bd* infection (Chatfield & Richards-Zawacki 2011, McMahon et al. 2014). Interestingly, high zoospore velocities persisted at temperatures well above the optimal ranges established for *Bd* growth rates in culture (Voyles et al. 2017, Sheets et al. 2021). Faster zoospores are likely to be better at infecting potential hosts (Canter & Jaworski 1981, Appiah et al. 2005), so our results suggest that *Bd* might be intrinsically better at infecting hosts at higher temperatures (not accounting for changes in host resistance; Raffel et al. 2013), at least until zoospores reach their CT_{max} and become immobile.

5. CONCLUSIONS

We found some evidence for curvilinear acclimation effects on maximum zoospore velocity when measured within 15 min of a temperature shift, consistent with the beneficial acclimation hypothesis. We found no clear effects of our experimental acclimation treatments on CT_{max}, but the presence of start temperature effects suggests that *Bd* zoospores might have undergone physiological acclimation within the 1–18 min it took to collect data following removal of zoospores from their acclimation treatments. Assuming these reflect real patterns of thermal plasticity, it is worth considering whether acclimation responses on this time scale might have any relevant effects on infection dynamics in amphibian hosts. The temperature variability hypothesis of Rohr & Raffel (2010) assumes that pathogens have either (1) constitutive thermal responses or (2) more rapid thermal acclimation responses than their hosts, following an unpredictable shift in temperature. Regardless of how one interprets our results, they are consistent with this assumption. These findings could have implications for climate change effects on *Bd* disease dynamics. If *Bd* zoospores are better equipped than their hosts to perform under variable temperature regimes due to either very rapid or constitutive thermal responses, then this effect might exacerbate chytrid-associated amphibian declines if climate conditions become more variable and unpredictable in the future (Raffel et al. 2013).

Data availability. Code and data can be accessed at https://github.com/huntercraig248/ZoosporeAcclimation

Acknowledgements. Funding for this study was provided by the National Science Foundation (IOS1651888). Frozen *Bd* stocks were provided by Joyce Longcore (University of Maine). Experimental assistance was provided by Jenna Agosta, Alejandro Hernandez, Sajjad Kamil, Declan McCrary, James Noelker, and Vanessa Six. Thank you to the Oakland University Department of Biological Sciences for TA support to H.M.C., J.P.S., and K.A.A; K.A.A. was also supported by a King-Parks-Chavez Future Faculty Fellowship while completing this work. The present work was part of H.M.C.'s PhD thesis.

LITERATURE CITED

Addy HD, Boswell EP, Koide RT (1998) Low temperature acclimation and freezing resistance of extraradical VA mycorrhizal hyphae. Mycol Res 102:582–586

Alcina A, Urzainqui A, Carrasco L (1988) The heat-shock response in *Trypanosoma cruzi.* Eur J Biochem 172:121–127

Allen JL, Clusella-Trullas S, Chown SL (2012) The effects of acclimation and rates of temperature change on critical thermal limits in *Tenebrio molitor* (Tenebrionidae) and *Cyrtobagous salviniae* (Curculionidae). J Insect Physiol 58:669–678

Altman KA, Paull SH, Johnson PTJ, Golembieski MN, Stephens JP, LaFonte BE, Raffel TR (2016) Host and parasite thermal acclimation responses depend on the stage of infection. J Anim Ecol 85:1014–1024

Angilletta MJ Jr (2009) Thermal adaptation: a theoretical and empirical synthesis. Oxford University Press, New York, NY

Appiah AA, van West P, Osborne MC, Gow NAR (2005) Potassium homeostasis influences the locomotion and encystment of zoospores of plant pathogenic oomycetes. Fungal Genet Biol 42:213–223

Arakelova KS (2001) The evaluation of individual production and scope for growth in aquatic sow bugs (*Asellus aquaticus*). Aquat Ecol 35:31–42

Bakthisaran R, Tangirala R, Rao ChM (2015) Small heat shock proteins: role in cellular functions and pathology. Biochim Biophys Acta Proteins Proteom 1854:291–319

Bennett AF, Lenski RE (1997) Evolutionary adaptation to temperature VI. Phenotypic acclimation and its evolution in *Escherichia coli.* Evolution 51:36–44

Bennett WA, McCauley RW, Beitinger TL (1998) Rates of gain and loss of heat tolerance in channel catfish. Trans Am Fish Soc 127:1051–1058

Boyle DG, Hyatt AD, Daszak P, Berger L and others (2003) Cryo-archiving of *Batrachochytrium dendrobatidis* and other chytridiomycetes. Dis Aquat Org 56:59–64

Brattstrom BH (1970) Thermal acclimation in Australian amphibians. Comp Biochem Physiol 35:69–103

Brattstrom BH, Lawrence P (1962) The rate of thermal acclimation in anuran amphibians. Physiol Zool 35:148–156

Brattstrom BH, Regal P (1965) Rate of thermal acclimation in the Mexican salamander *Chiropterotriton.* Copeia 1965: 514–515

Brown JH, Gillooly JF, Allen AP, Savage VM, West GB (2004) Toward a metabolic theory of ecology. Ecology 85: 1771–1789

Bruce RC (2022) Size and cycle in dusky salamanders. J Herpetol 56:444–453

Canter HM, Jaworski GHM (1981) The effect of light and darkness upon infection of *Asterionella formosa* Hassall by the chytrid *Rhizophydium planktonicum* Canter emend. Ann Bot 47:13–30

Carilo Filho LM, Gomes L, Katzenberger M, Solé M, Orrico VGD (2022) There and back again: a meta-analytical approach on the influence of acclimation and altitude in the upper thermal tolerance of amphibians and reptiles. Front Ecol Evol 10:1017255

Chatfield MWH, Richards-Zawacki CL (2011) Elevated temperature as a treatment for *Batrachochytrium dendrobatidis* infection in captive frogs. Dis Aquat Org 94:235–238

Chung KS (1981) Rate of acclimation of the tropical salt-marsh fish *Cyprinodon dearborni* to temperature changes. Hydrobiologia 78:177–181

Claussen DL (1977) Thermal acclimation in ambystomatid salamanders. Comp Biochem Physiol Part A Physiol 58: 333–340

Claussen DL (1980) Thermal acclimation in the crayfish, *Orconectes rusticus* and *O. virilis.* Comp Biochem Physiol Part A Physiol 66:377–384

Cohen LM, Neimark H, Eveland LK (1980) *Schistosoma mansoni*: response of cercariae to a thermal gradient. J Parasitol 66:362–364

Cossins AR, Friedlander MJ, Prosser CL (1977) Correlations between behavioral temperature adaptations of goldfish and the viscosity and fatty acid composition of their synaptic membranes. J Comp Physiol 120:109–121

Crowther TW, Bradford MA (2013) Thermal acclimation in widespread heterotrophic soil microbes. Ecol Lett 16: 469–477

Dell AI, Pawar S, Savage VM (2013) The thermal dependence of biological traits. Ecological Archives E094–108. Ecology 94:1205

Dell AI, Pawar S, Savage VM (2014) Temperature dependence of trophic interactions are driven by asymmetry of species responses and foraging strategy. J Anim Ecol 83: 70–84

Engstler M, Boshart M (2004) Cold shock and regulation of surface protein trafficking convey sensitization to inducers of stage differentiation in *Trypanosoma brucei.* Genes Dev 18:2798–2811

Fang J, McCutchan TF (2002) Thermoregulation in a parasite's life cycle. Nature 418:742

Fangue NA, Wunderly MA, Dabruzzi TF, Bennett WA (2014) Asymmetric thermal acclimation responses allow sheepshead minnow *Cyprinodon variegatus* to cope with rapidly changing temperatures. Physiol Biochem Zool 87: 805–816

Fargues J, Goettel MS, Smits N, Ouedraogo A, Rougier M (1997) Effect of temperature on vegetative growth of *Beauveria bassiana* isolates from different origins. Mycologia 89:383–392

Farrer RA, Weinert LA, Bielby J, Garner TWJ and others (2011) Multiple emergences of genetically diverse amphibian-infecting chytrids include a globalized hypervirulent recombinant lineage. Proc Natl Acad Sci USA 108:18732–18736

Finkelstein DB, Strausberg S (1982) Expression of a cloned yeast heat-shock gene. In: Schlesinger MJ, Ashburner M, Tissières A (eds) Heat shock from bacteria to man. Cold Spring Harbor Laboratory, Cold Spring Harbor, NY, p 63–68

Fitzpatrick LC (1973) Influence of seasonal temperatures on the energy budget and metabolic rates of the northern two-lined salamander *Eurycea bislineata bislineata*. Comp Biochem Physiol Part A Physiol 45:807–818

Fox J, Weisberg S (2019) An R companion to applied regression, 3rd edn. Sage, Thousand Oaks, CA

Gatz RN, Piiper J (1979) Anaerobic energy metabolism during severe hypoxia in the lungless salamander *Desmognathus fuscus* (Plethodontidae). Respir Physiol 38: 377–384

Gillooly JF, Brown JH, West GB, Savage VM, Charnov EL (2001) Effects of size and temperature on metabolic rate. Science 293:2248–2251

Hall EK, Singer GA, Kainz MJ, Lennon JT (2010) Evidence for a temperature acclimation mechanism in bacteria: an empirical test of a membrane-mediated trade-off. Funct Ecol 24:898–908

Heinemeyer A, Ineson P, Ostle N, Fitter AH (2006) Respiration of the external mycelium in the arbuscular mycorrhizal symbiosis shows strong dependence on recent photosynthates and acclimation to temperature. New Phytol 171:159–170

Huey RB, Berrigan D, Gilchrist GW, Herron JC (1999) Testing the adaptive significance of acclimation: a strong inference approach. Am Zool 39:323–336

Hutchison VH (1961) Critical thermal maxima in salamanders. Physiol Zool 34:92–125

Hutchison VH, Ferrance MR (1970) Thermal tolerances of *Rana pipiens* acclimated to daily temperature cycles. Herpetologica 26:1–8

Hutchison VH, Rowlan SD (1975) Thermal acclimation and tolerance in the mudpuppy, *Necturus maculosus.* J Herpetol 9:367–368

Hutchison VH, Engbretson G, Turney D (1973) Thermal acclimation and tolerance in the hellbender, *Cryptobranchus alleganiensis.* Copeia 1973:805–807

Ikwegbue PC, Masamba P, Oyinloye BE, Kappo AP (2017) Roles of heat shock proteins in apoptosis, oxidative stress, human inflammatory diseases, and cancer. Pharmaceuticals 11:2

Kalinina LV, Khrebtukova IA, Podgornaya OL, Wasik A, Sikora J (1988) Heat shock proteins in Amoeba. Eur J Protistol 24:64–68

Kingsolver JG, Umbanhowar J (2018) The analysis and interpretation of critical temperatures. J Exp Biol 221:jeb167858

Krobitsch S, Brandau S, Hoyer C, Schmetz C, Hübel A, Clos J (1998) *Leishmania donovani* Heat Shock Protein 100. J Biol Chem 273:6488–6494

Kumar R, Malagon DA, Carter ED, Miller DL and others (2020) Experimental methodologies can affect pathogenicity of *Batrachochytrium salamandrivorans* infections. PLOS ONE 15:e0235370

Lagerspetz KYH, Bowler K (1993) Variation in heat tolerance in individual *Asellus aquaticus* during thermal acclimation. J Therm Biol 18:137–143

Layne JR Jr, Claussen DL (1982a) Seasonal variation in the thermal acclimation of critical thermal maxima (CTMax) and minima (CTMin) in the salamander *Eurycea bislineata.* J Therm Biol 7:29–33

Layne JR Jr, Claussen DL (1982b) The time courses of CTMax and CTMin acclimation in the salamander *Desmognathus fuscus.* J Therm Biol 7:139–141

Lienhard JH IV, Lienhard JH V (2020) A heat transfer textbook, 5th edn. Phlogiston Press, Cambridge, MA

Longcore JE, Pessier AP, Nichols DK (1999) *Batrachochytrium dendrobatidis* gen. et sp. nov., a chytrid pathogenic to amphibians. Mycologia 91:219–227

Loomis WF, Wheeler SA (1982) The physiological role of heat-shock proteins in Dictyostelium. In: Schlesinger MJ, Ashburner M, Tissières A (eds) Heat shock from bacteria to man. Cold Spring Harbor Laboratory, Cold Spring Harbor, NY, p 353–359

Lutterschmidt WI, Hutchison VH (1997) The critical thermal maximum: history and critique. Can J Zool 75:1561–1574

Malcolm GM, López-Gutiérrez JC, Koide RT, Eissenstat DM (2009) Acclimation to temperature and temperature sensitivity of metabolism by ectomycorrhizal fungi. Glob Change Biol 15:2333

McMahon TA, Sears BF, Venesky MD, Bessler SM and others (2014) Amphibians acquire resistance to live and dead fungus overcoming fungal immunosuppression. Nature 511:224–227

McWhinnie RB, Sckrabulis JP, Raffel TR (2021) Temperature and mass scaling affect cutaneous and pulmonary respiratory performance in a diving frog. Integr Zool 16:712–728

Molnár PK, Sckrabulis JP, Altman KA, Raffel TR (2017) Thermal performance curves and the metabolic theory of ecology—a practical guide to models and experiments for parasitologists. J Parasitol 103:423–439

Neidhardt FC, VanBogelen RA, Lau ET (1982) The high-temperature regulon of *Escherichia coli.* In: Schlesinger MJ, Ashburner M, Tissières A (eds) Heat shock from bacteria to man. Cold Spring Harbor Laboratory, Cold Spring Harbor, NY, p 139–145

Nickerson MA, Mays CE (1973) A study of the Ozark hellbender *Cryptobranchus alleganiensis bishopi.* Ecology 54:1164–1165

Oliveira BF, São-Pedro VA, Santos-Barrera G, Penone C, Costa GC (2017) AmphiBIO, a global database for amphibian ecological traits. Sci Data 4:170123

Ouedraogo A, Fargues J, Goettel MS, Lomer CJ (1997) Effect of temperature on vegetative growth among isolates of *Metarhizium anisopliae* and *M. flavoviride.* Mycopathologia 137:37–43

Pedersen JS (2011) wrMTrck. www.phage.dk/plugins/wrmtrck.html

Pellon JR, Gomez RF, Sinskey AJ (1982) Association of the *Escherichia coli* nucleoid with protein synthesized during thermal treatments. In: Schlesinger MJ, Ashburner M, Tissières A (eds) Heat shock from bacteria to man. Cold Spring Harbor Laboratory, Cold Spring Harbor, NY, p 121–125

Piotrowski JS, Annis SL, Longcore JE (2004) Physiology of *Batrachochytrium dendrobatidis*, a chytrid pathogen of amphibians. Mycologia 96:9–15

Pottier P, Lin HY, Oh RRY, Pollo P and others (2022) A comprehensive database of amphibian heat tolerance. Sci Data 9:600

R Core Team (2020) R: a language and environment for statistical computing. R Foundation for Statistical Computing, Vienna

Rabb GB (1958) On certain Mexican salamanders of the plethodontid genus *Chiropterotriton*. Occas Pap Mus Zool Univ Mich 587:1–37

Raffel TR, Romansic JM, Halstead NT, McMahon TA, Venesky MD, Rohr JR (2013) Disease and thermal acclimation in a more variable and unpredictable climate. Nat Clim Change 3:146–151

Raffel TR, Halstead NT, McMahon TA, Davis AK, Rohr JR (2015) Temperature variability and moisture synergistically interact to exacerbate an epizootic disease. Proc R Soc B 282:20142039

Robinson CH (2001) Cold adaptation in Arctic and Antarctic fungi. New Phytol 151:341–353

Robinson PM, Morris GM (1984) Tolerance of hyphae of *Fusarium oxysporum* f. sp. *lycopersici* to low temperature. Trans Br Mycol Soc 83:569–573

Rohr JR, Raffel TR (2010) Linking global climate and temperature variability to widespread amphibian declines putatively caused by disease. Proc Natl Acad Sci USA 107:8269–8274

Rohr JR, Civitello DJ, Cohen JM, Roznik EA, Sinervo B, Dell AI (2018) The complex drivers of thermal acclimation and breadth in ectotherms. Ecol Lett 21:1425–1439

Schlesinger MJ, Ashburner M, Tissières A (eds) (1982) Heat shock from bacteria to man. Cold Spring Harbor Laboratory, Cold Spring Harbor, NY

Schneider CA, Rasband WS, Eliceiri KW (2012) NIH Image to ImageJ: 25 years of image analysis. Nat Methods 9: 671–675

Sheets CN, Schmidt DR, Hurtado PJ, Byrne AQ, Rosenblum EB, Richards-Zawacki CL, Voyles J (2021) Thermal performance curves of multiple isolates of *Batrachochytrium dendrobatidis*, a lethal pathogen of amphibians. Front Vet Sci 8:687084

Sherman E, Levitis D (2003) Heat hardening as a function of developmental stage in larval and juvenile *Bufo americanus* and *Xenopus laevis.* J Therm Biol 28:373–380

Spotila JR, Standora EA, Easton DP, Rutledge PS (1989) Bioenergetics, behavior, and resource partitioning in stressed habitats: biophysical and molecular approaches. Physiol Zool 62:253–285

Stevenson LA, Alford RA, Bell SC, Roznik EA, Berger L, Pike DA (2013) Variation in thermal performance of a widespread pathogen, the amphibian chytrid fungus *Batrachochytrium dendrobatidis.* PLOS ONE 8:e73830

Szczerbowski JA (2001) *Carassius auratus* (Linneaus, 1758). In: Bănărescu PM, Paepke HJ (eds) The freshwater fishes of Europe: Cyprinidae 2 part III. *Carassius* to *Cyprinus.* Gasterosteidae. Aula-Verlag, Wiebelsheim, p 5–41

Terblanche JS, Deere JA, Clusella-Trullas S, Janion C, Chown SL (2007) Critical thermal limits depend on methodological context. Proc R Soc B 274:2935–2942

Therneau TM (2001) survival: survival analysis. R package version 3.7–0. https://CRAN.R-project.org/package=survival

Tian W, Sun H, Zhang Y, Xu J and others (2022) Thermal adaptation occurs in the respiration and growth of widely distributed bacteria. Glob Change Biol 28:2820–2829

Travers A, Mace H (1982) The heat-shock phenomenon in bacteria — a protection against DNA relaxation? In: Schlesinger MJ, Ashburner M, Tissières A (eds) Heat shock from bacteria to man. Cold Spring Harbor Laboratory, Cold Spring Harbor, NY, p 127–130

Tsukuda H (1960) Temperature adaptation in fishes IV. Change in the heat and cold tolerances of the guppy in the process of temperature acclimatization. J Inst Polytech D11:43–54

Tveit AT, Söllinger A, Rainer EM, Didriksen A and others (2023) Thermal acclimation of methanotrophs from the genus *Methylobacter.* ISME J 17:502–513

Urrejola S, Nespolo R, Lardies MA (2011) Diet-induced developmental plasticity in life histories and energy metabolism in a beetle. Rev Chil Hist Nat 84:523–533

Vidal C, Fargues J, Lacey LA (1997) Intraspecific variability of *Paecilomyces fumosoroseus*: effect of temperature on vegetative growth. J Invertebr Pathol 70:18–26

Voyles J, Johnson LR, Briggs CJ, Cashins SD and others (2014) Experimental evolution alters the rate and temporal pattern of population growth in *Batrachochytrium dendrobatidis*, a lethal fungal pathogen of amphibians. Ecol Evol 4:3633–3641

Voyles J, Johnson LR, Rohr J, Kelly R and others (2017) Diversity in growth patterns among strains of the lethal fungal pathogen *Batrachochytrium dendrobatidis* across extended thermal optima. Oecologia 184:363–373

Wilson RS, Franklin CE (2002) Testing the beneficial acclimation hypothesis. Trends Ecol Evol 17:66–70

Woodhams DC, Alford RA, Briggs CJ, Johnson M, Rollins-Smith LA (2008) Life-history trade-offs influence disease in changing climates: strategies of an amphibian pathogen. Ecology 89:1627–1639

Yamamori T, Osawa T, Tobe T, Ito K, Yura T (1982) *Escherichia coli* gene (hin) controls transcription of heat-shock operons and cell growth at high temperature. In: Schlesinger MJ, Ashburner M, Tissières A (eds) Heat shock from bacteria to man. Cold Spring Harbor Laboratory, Cold Spring Harbor, NY, p 131–137

Zaibel I, Appelbaum Y, Arnon S, Britzi M, Schwartsburd F, Snyder S, Zilberg D (2019) The effect of tertiary treated wastewater on fish growth and health: laboratory-scale experiment with *Poecilia reticulata* (guppy). PLOS ONE 14:e0217927

Editorial responsibility: Douglas Woodhams, Boston, Massachusetts, USA
Reviewed by: 3 anonymous referees

Submitted: February 17, 2024
Accepted: October 16, 2024
Proofs received from author(s): November 26, 2024